

## SEARCHES FOR HIGGS BOSONS

Written February 2000 by P. Igo-Kemenes (Physikalisches Institut, Heidelberg, Germany)

### I. Introduction

One of the main challenges in high energy physics is the discovery of Higgs bosons. Their existence is related to the generation of elementary particle masses. In the Standard Model (SM) [1], the electroweak interaction is described by a gauge field theory based on the  $SU(2)_L \times U(1)_Y$  symmetry group. Masses can be introduced by the Higgs mechanism [2], where fundamental scalar “Higgs” fields interact with each other such that they acquire a nonzero vacuum expectation value and the  $SU(2)_L \times U(1)_Y$  symmetry is spontaneously broken down to the electromagnetic  $U(1)_{EM}$  symmetry. Gauge bosons and fermions obtain their masses by interacting with the vacuum Higgs field. Associated with this mechanism is the existence of massive scalar particles called Higgs bosons, and the proof for the above mechanism would come from the direct observation of this novel particle species.

In its minimal version, the SM requires one Higgs field doublet and predicts a single neutral Higgs boson. Beyond the SM, supersymmetric (SUSY) models [3] are considered. They provide a consistent framework for the unification of the gauge interactions at a high energy scale  $\Lambda_{GUT} \approx 10^{16}$  GeV and an explanation for the stability of the electroweak energy scale in the presence of quantum corrections (the “scale hierarchy problem”). Moreover, their predictions are compatible with existing high-precision data. The Minimal Supersymmetric Standard Model (MSSM) [4] is the SUSY extension of the SM with minimal new particle content. It needs two Higgs field doublets and predicts the existence of three neutral and a pair of charged Higgs bosons. While in the SM the mass of the Higgs boson is not predicted, in SUSY models the Higgs masses are related to the gauge couplings. As a consequence, one of the neutral Higgs bosons must have its mass close to the electroweak energy scale. In the MSSM this mass is predicted to be less than about 135 GeV [5].

Prior to 1989, when the  $e^+e^-$  collider LEP at CERN came into operation, Higgs boson searches were sensitive to masses below a few GeV only (see Ref. 6 for a review). The LEP collider, operating for five years at a center-of-mass energy  $\sqrt{s} \approx M_{Z^0}$  (the LEP1 phase), definitively excluded a SM Higgs boson with a mass between zero and about 65 GeV [7]. Since 1995, the center-of-mass energy has increased each year (the LEP2 phase) and has reached  $\sqrt{s} = 204$  GeV in 1999, within a few GeV of the highest energy expected. When the full data of the four LEP experiments are combined, the sensitivity for discovery will extend to SM Higgs boson masses of approximately 110 GeV. After the LEP experiments finish taking data, searches for Higgs bosons will be pursued primarily at the Tevatron  $p\bar{p}$  collider. The sensitivity to Higgs bosons in the Run I data is rather limited, though the planned energy and luminosity upgrades (Run II [8]) would extend the sensitivity well beyond the LEP range. The searches will continue later at the LHC  $pp$  collider [9] covering the canonical mass range up to about 1 TeV. If Higgs bosons are discovered, the Higgs mechanism can be studied in great detail at future  $e^+e^-$  [10] and  $\mu^+\mu^-$  colliders [11].

The sensitivity of current searches is continuously improving with increasing collider energies and sample sizes. There is also ongoing activity in refining the phenomenology relevant to Higgs boson searches. In order to provide an up to date description, recent documents are quoted even though in some cases they are not published. Such documents (indicated by *\*name\** in the Reference list) can be accessed conveniently from the web page <http://home.cern.ch/p/pik/www/pdg2000/index.html>.

## II. Higgs boson masses

*In the Standard Model*, the Higgs mass  $m_{H^0} = \sqrt{2\lambda} v$  is proportional to the vacuum expectation value  $v$  of the Higgs field, which is fixed by the Fermi coupling. The quartic Higgs coupling  $\lambda$ , and thus  $m_{H^0}$ , is not determined, but arguments of self-consistency of the theory can be used to place upper and lower bounds on  $m_{H^0}$ .

Since the running coupling  $\lambda$  rises indefinitely with energy, the theory would eventually become non-perturbative. The requirement that in the SM this does not occur at a scale lower than  $\Lambda$  defines an upper bound for the Higgs mass [12]. On the other hand, a lower bound for  $m_{H^0}$  is obtained from top-loop induced quantum corrections to the Higgs interaction potential [13]. The requirement that the electroweak minimum is an absolute minimum up to the scale  $\Lambda$  yields a “vacuum stability” condition which limits  $m_{H^0}$  from below. These theoretical bounds are summarized in Fig. 1 [14] as a function of  $\Lambda$ . Self-consistency of the SM up to  $\Lambda = \Lambda_{\text{GUT}}$  allows only the narrow band from about 130 to 190 GeV for the mass. This range is beyond the reach of LEP2, which implies that the discovery of a Higgs boson at LEP would indicate new physics beyond the SM at energies lower than  $\Lambda_{\text{GUT}}$ .

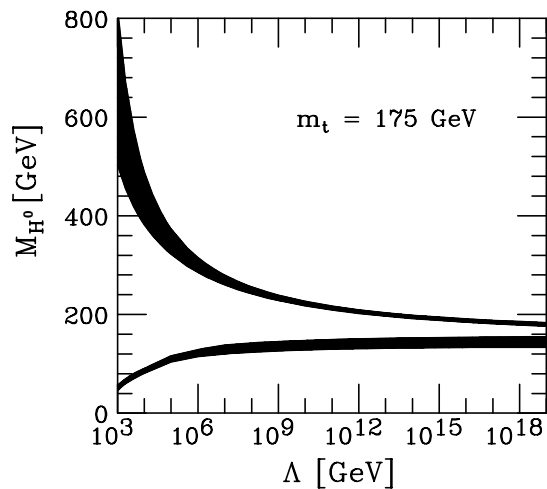


**Figure 1:** Bounds on the Higgs mass based on arguments of self-consistency of the SM [14].  $\Lambda$  denotes the energy scale at which the SM would become non-perturbative or the electroweak potential unstable. The dark bands represent theoretical uncertainties.

Indirect experimental bounds for the Higgs mass are obtained from fits to precision measurements of electroweak observables, primarily from  $Z^0$  decay data, and to the measured top and  $W^\pm$  masses [15]. These measurements are sensitive to  $\log(m_{H^0})$  through radiative corrections. Currently the best fit value is  $m_{H^0} = 77_{-39}^{+69}$  GeV, and  $m_{H^0} < 215$  GeV is obtained at the 95% confidence level (CL) [16], still consistent with the SM being valid up to the GUT scale.

*In the MSSM*, one of the two Higgs field doublets, with vacuum expectation value  $v_1$ , couples to “down” quarks and charged leptons while the second, with  $v_2$ , couples to “up” quarks only. Assuming  $CP$  invariance, the spectrum of physical Higgs bosons [4] consists of two  $CP$ -even neutral scalars  $h^0$  and  $H^0$  ( $h^0$  is the one with the smaller mass), one  $CP$ -odd neutral scalar  $A^0$ , and one pair of charged Higgs bosons  $H^\pm$ .

At the tree level, only two parameters are required (beyond the  $Z^0$  mass) to fix all Higgs masses and couplings. A convenient choice is the ratio  $\tan\beta = v_2/v_1$  and the mass ( $m_{A^0}$ ) of the  $CP$ -odd scalar  $A^0$ . The mixing angle  $\alpha$  which diagonalizes the  $CP$ -even Higgs mass matrix can also be expressed in terms of  $\tan\beta$  and  $m_{A^0}$ . The following ordering of masses is valid at the tree level:  $m_{h^0} < M_Z$ ,  $m_{A^0} < m_{H^0}$ , and  $m_{A^0}, M_W < m_{H^\pm}$ . These relations are modified by radiative corrections; the largest contribution is a consequence of the incomplete cancelation between virtual-top and scalar-top (stop) loops. The corrections affect mainly the masses and decay branching ratios in the neutral Higgs sector. They depend strongly on the top quark mass ( $\sim m_t^4$ ) and logarithmically on the stop masses, and involve a detailed parameterization of SUSY breaking and of the mixing between the SUSY partners of the left- and right-handed top quarks [17].

The Higgs masses, after radiative corrections, are displayed in Fig. 2 as a function of  $m_{A^0}$  for two representative values of  $\tan\beta$  within the range from 1 to  $\approx m_t/m_b$  which is preferred in grand unification schemes [18]. One observes that  $m_{h^0}$  may exceed  $M_Z$ .

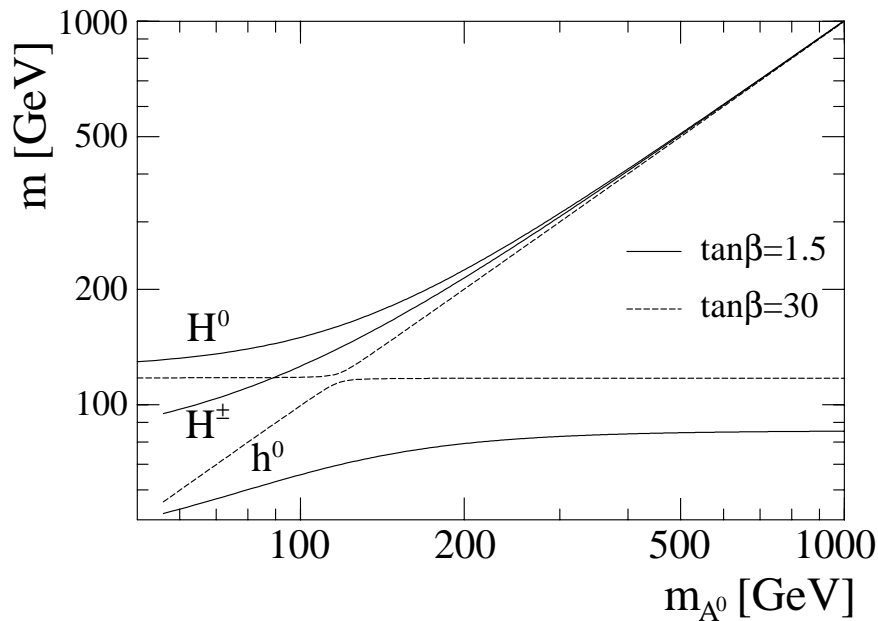


**Figure 2:** Higgs masses in the MSSM after radiative corrections, as a function of  $m_{A^0}$  for two representative values of  $\tan\beta$ ; 1.5 and 30 (in the case of  $H^\pm$  the variation with  $\tan\beta$  is invisible on the scale of the figure).

### III. Higgs boson production and decay

A comprehensive discussion of the Higgs boson phenomenology is given in Ref. 19. In this section the focus is on Higgs production in  $e^+e^-$  collisions at energies below 210 GeV (LEP2) [20] by which most of the recent search results have been obtained. Extensions to higher  $e^+e^-$  energies [10] and to production in hadron collisions [8,9] are discussed briefly in Sections V and VI.

#### *Higgs boson production in $e^+e^-$ collisions:*

The principal mechanism for producing the **SM Higgs particle** in  $e^+e^-$  collisions at current energies is Higgs-strahlung in the  $s$ -channel [21],  $e^+e^- \rightarrow H^0 Z^0$ , where a Higgs boson is radiated off an intermediate  $Z^0$  boson. The  $Z^0$  boson in the final state is either virtual (LEP1) or on the mass shell (LEP2). In the latter case (at energies far from the  $Z^0$  resonance) the cross section is given by

$$\sigma(e^+e^- \rightarrow Z^0 H^0) = \frac{G_F^2 M_Z^4}{96\pi s} (v_e^2 + a_e^2) \lambda^{1/2} \frac{\lambda + 12M_Z^2/s}{(1 - M_Z^2/s)^2} \equiv \sigma_{\text{SM}} \quad (1)$$

where  $s$  denotes the center-of-mass energy squared,  $a_e = -1$ ,  $v_e = -1 + 4s_W^2$  ( $s_W = \sin \theta_W$  is the *sine* of the weak-mixing angle), and  $\lambda = [1 - (m_{H^0} + M_Z)^2/s][1 - (m_{H^0} - M_Z)^2/s]$  is the two-particle phase-space function. The cross section [21,22] is shown in Fig. 3 as a function of  $\sqrt{s}$ , together with that of other SM processes.

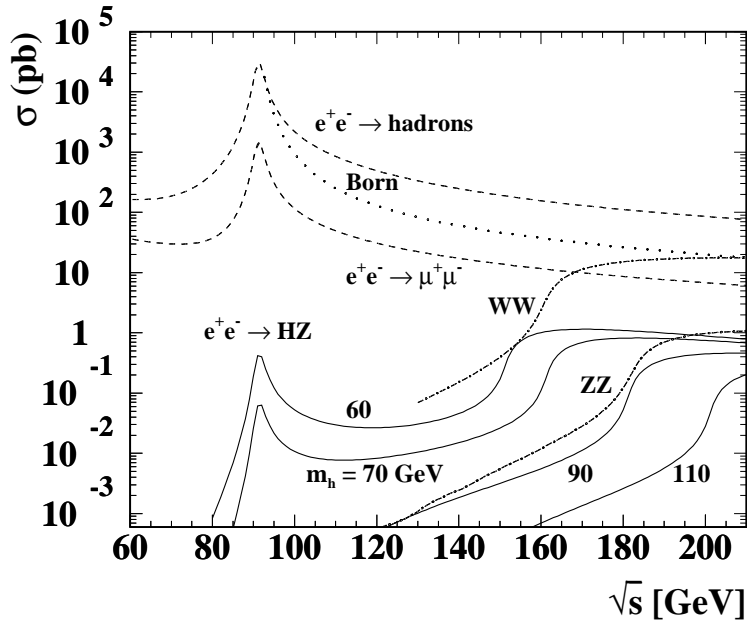


**Figure 3:** Cross sections for the Higgs-strahlung process in the SM for fixed values of  $m_{H^0}$  (full lines) and for other SM processes which contribute to the background, as a function of  $\sqrt{s}$ .

The SM Higgs boson can also be produced by  $W^+W^-$  fusion in the  $t$ -channel [23],  $e^+e^- \rightarrow \bar{\nu}_e \nu_e H^0$ , but at current energies this process has a small contribution to the cross section, except for Higgs masses which cannot be reached by the Higgs-strahlung process. The  $W^+W^-$  fusion process may extend slightly the ultimate range of sensitivity at LEP2 [20].

*In the MSSM*, the main production mechanisms of the neutral Higgs bosons  $h^0$  and  $A^0$  are [24] the Higgs-strahlung process  $e^+e^- \rightarrow h^0 Z^0$  and the pair-production process  $e^+e^- \rightarrow h^0 A^0$ . As in the SM case, the fusion process plays a marginal role at current energies. Furthermore, the production of the heavy neutral  $CP$ -even Higgs boson  $H^0$  is suppressed over most of the parameter space currently accessible. The cross sections for the Higgs-strahlung and pair-production processes may be expressed in terms of  $\sigma_{\text{SM}}$  given in Eq. (1) and the angles  $\alpha$  and  $\beta$  introduced before:

$$\sigma(e^+e^- \rightarrow Z^0 h^0) = \sin^2(\beta - \alpha)\sigma_{\text{SM}} \quad (2)$$

$$\sigma(e^+e^- \rightarrow A^0 h^0) = \cos^2(\beta - \alpha)\bar{\lambda}\sigma_{\text{SM}} , \quad (3)$$

with the kinematic factor  $\bar{\lambda} = \lambda_{A^0 h^0}^{3/2} / [\lambda_{Z^0 h^0}^{1/2} (12M_Z^2/s + \lambda_{Z^0 h^0})]$  and  $\lambda_{ij} = [1 - (m_i + m_j)^2/s][1 - (m_i - m_j)^2/s]$ . The cross sections are complementary due to the MSSM suppression factors  $\sin^2(\beta - \alpha)$  and  $\cos^2(\beta - \alpha)$ . At small  $\tan\beta$  the process  $e^+e^- \rightarrow Z^0 h^0$  has the larger cross section while at large  $\tan\beta$  it is  $e^+e^- \rightarrow h^0 A^0$ , unless the latter is suppressed kinematically.

In models with *two Higgs field doublets* (2HD models), including the MSSM, charged Higgs bosons are expected to be produced in pairs [19,25],  $e^+e^- \rightarrow H^+H^-$ , and the cross section is fixed at the tree level by the mass  $m_{H^\pm}$ :

$$\begin{aligned} \sigma(e^+e^- \rightarrow H^+H^-) &= \frac{2G_F^2 M_W^4 s_W^4}{3\pi s} \\ &\times \left[ 1 + \frac{v_e v_H}{4s_W^2 c_W^2 (1 - M_Z^2/s)} + \frac{(a_e^2 + v_e^2)v_H^2}{64s_W^4 c_W^4 (1 - M_Z^2/s)^2} \right] \beta_H^3 \quad (4) \end{aligned}$$

with  $c_W = \cos\theta_W$ ,  $v_H = -1 + 2s_W^2$ , and  $\beta_H = (1 - 4m_{H^\pm}^2/s)^{1/2}$ .

### **Higgs boson decay:**

In the case of the *SM Higgs boson*, the most relevant decay branching ratios [22,26] are summarized in Fig. 4. For masses below about 135 GeV, decays to fermion anti-fermion pairs dominate, and  $H^0 \rightarrow b\bar{b}$  has the largest branching ratio. Decays to  $\tau^+\tau^-$ ,  $c\bar{c}$ , and gluon pairs (*via* loops) are below

10%. The decay width is less than 10 MeV. For larger masses, the  $W^+W^-$ ,  $Z^0Z^0$  final states dominate [10] and the decay width rises rapidly with mass, reaching about 1 GeV for  $m_{H^0} = 200$  GeV and 100 GeV for  $m_{H^0} = 500$  GeV.

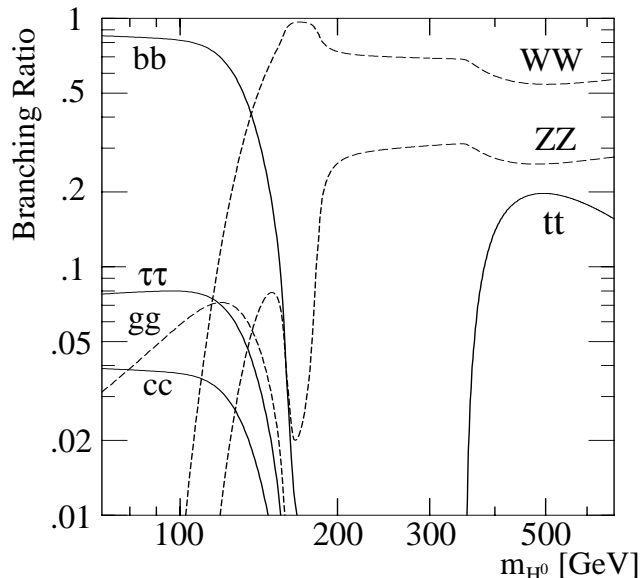


**Figure 4:** Branching ratios for the main decay modes of the SM Higgs boson [10].

*In the MSSM*, the couplings of the neutral Higgs bosons to quarks, leptons, and gauge bosons are modified with respect to those of the SM Higgs boson by factors which depend upon the mixing angles  $\alpha$  and  $\beta$ . These factors, valid at leading order, are summarized in Table 1. The decays are discussed in [19,24]. Some features relevant to current searches are discussed below.

- The  $h^0$  boson will decay mainly to fermion pairs since the mass is smaller than about 135 GeV. The  $A^0$  boson also decays predominantly to fermion pairs, independently of its mass, since its coupling to vector bosons is zero at leading order (see Table 1). For  $\tan\beta > 1$ , decays to  $b\bar{b}$  and  $\tau^+\tau^-$  pairs are preferred, with branching ratios of about 90% and 8%, respectively, while the decays to  $c\bar{c}$  and gluon

**Table 1:** Factors relating the SM Higgs couplings to the corresponding couplings in the MSSM.

	“Up” fermions	“Down” fermions	Vector bosons
SM-Higgs:	1	1	1
MSSM $h^0$ :	$\cos \alpha / \sin \beta$	$-\sin \alpha / \cos \beta$	$\sin(\beta - \alpha)$
$H^0$ :	$\sin \alpha / \sin \beta$	$\cos \alpha / \cos \beta$	$\cos(\beta - \alpha)$
$A^0$ :	$1 / \tan \beta$	$\tan \beta$	0

pairs are suppressed. Decays to  $c\bar{c}$  may become important for  $\tan \beta < 1$ .

- The decay  $h^0 \rightarrow A^0 A^0$  may become dominant if it is kinematically allowed [25].
- Other possible decays are into SUSY particles such as sfermions, charginos or neutralinos, which may lead to invisible or barely visible final states. The branching fractions can be large, even dominant in parts of the MSSM parameter space, thus requiring a different search strategy.

**Charged Higgs bosons** in 2HD models decay mainly *via*  $H^+ \rightarrow \tau^+ \nu_\tau$  if  $\tan \beta$  is large. For small  $\tan \beta$ , the decay to  $c\bar{s}$  is dominant at low mass, and the decay to  $H^+ \rightarrow t^* \bar{b} \rightarrow W^+ b \bar{b}$  is dominant for  $H^\pm$  masses larger than about 130 GeV [27].

#### IV. The search environment at LEP

During the first phase of LEP, the experiments ALEPH, DELPHI, L3, and OPAL analysed over four million  $Z^0$  decays each. They have set lower bounds of approximately 65 GeV on the mass of the SM Higgs boson, and of about 45 GeV on the masses of the  $h^0$ ,  $A^0$  (valid for  $\tan \beta > 1$ ) and also for  $H^\pm$  bosons. At energies above the  $Z^0$  resonance (the LEP2 phase) the experimental environment is different in many respects. The signal-to-background ratio at LEP2 is more favorable (see Fig. 3), despite the additional backgrounds from the processes  $e^+e^- \rightarrow W^+W^-$  and  $Z^0Z^0$ . The latter have kinematic properties similar to the signal process  $e^+e^- \rightarrow H^0Z^0$ , but since

at LEP2 the  $Z^0$  boson is on the mass shell, constrained kinematic fits allow a good overall signal-to-background ratio to be achieved. Furthermore, since neutral Higgs bosons decay preferentially to  $b\bar{b}$ , the LEP Collaborations have considerably upgraded their  $b$ -tagging capabilities for the LEP2 phase. Jets with  $B$  hadrons are recognized by the presence of secondary decay vertices or tracks with large impact parameters, identified by means of high-precision silicon microvertex detectors. Other indicators for  $B$  hadron decays are high- $p_T$  leptons ( $\ell = e, \mu$ ) from  $b \rightarrow c\ell^-\bar{\nu}_\ell$  decays and several jet properties.

The following final states provide good sensitivity for neutral Higgs bosons (here  $h^0$  may designate either the SM Higgs boson or the light  $CP$ -even neutral scalar in the MSSM).

(a) The **four-jet final state** is produced by the processes  $(h^0 \rightarrow b\bar{b})(Z^0 \rightarrow q\bar{q})$  and  $(h^0 \rightarrow b\bar{b})(A^0 \rightarrow b\bar{b})$ . In the SM it occurs with a branching ratio of 58%. In the first process, the invariant mass of two of the jets is close to  $M_Z$ , while the other two jets contain  $B$  hadrons. In the second process, the  $Z^0$  mass constraint cannot be used, but  $B$  hadrons are expected in all four jets. The Higgs mass can be reconstructed with a typical resolution of 2.5 GeV.

(b) The **missing-energy final state** is produced mainly by the process  $(h^0 \rightarrow b\bar{b})(Z^0 \rightarrow \nu\bar{\nu})$ . In the SM it occurs with a branching ratio of 17%. The signal has two jets with  $B$  hadrons, substantial missing transverse momentum and missing mass compatible with  $M_Z$ . A similar event topology would also occur in  $h^0 Z^0$  and  $h^0 A^0$  if the  $h^0$  or the  $A^0$  boson decayed into “invisible” SUSY particles (*e.g.*, neutralinos), or in the  $W^+W^-$  fusion process leading to  $b\bar{b}\nu_e\bar{\nu}_e$  events. The reconstruction of the Higgs boson requires good knowledge of the detector acceptance and energy resolution; it is achieved with a typical resolution of 3 GeV, but the distribution usually has a pronounced non-Gaussian tail.

(c) The **leptonic final states** are produced in the processes  $(h^0 \rightarrow b\bar{b})(Z^0 \rightarrow e^+e^-, \mu^+\mu^-)$ . In the SM the branching ratios add up to 6%. The two leptons reconstruct to  $M_Z$  and the two jets contain  $B$  hadrons. Although the branching ratio is small, this channel adds considerably to the overall search sensitivity

since it has low background and good mass resolution, typically 1.5 GeV, if  $m_{h^0}$  is taken to be the mass recoiling against the reconstructed  $Z^0$  boson.

(d) The *tau final states* are produced in the SM and MSSM processes  $(h^0 \rightarrow \tau^+\tau^-)(Z^0 \rightarrow q\bar{q})$ ,  $(h^0 \rightarrow q\bar{q})(Z^0 \rightarrow \tau^+\tau^-)$ ,  $(h^0 \rightarrow \tau^+\tau^-)(A^0 \rightarrow q\bar{q})$ , and  $(h^0 \rightarrow q\bar{q})(A^0 \rightarrow \tau^+\tau^-)$ . In the SM they occur with a branching ratio of about 10% in total. These channels play an important role in some subsets of the MSSM parameter space where the decays to  $b\bar{b}$  are suppressed.

To summarize, the conjunction of constrained kinematic fits and sophisticated  $b$  tagging allows the searches at LEP2 to be conducted with increased sensitivity. With the inclusion of the abundant four-jet final states, which had to be discarded at LEP1 from searches for the SM Higgs boson, about 95% of the signal cross section is utilized.

Searches for the charged Higgs process  $e^+e^- \rightarrow H^+H^-$  make use of the decays  $H^+ \rightarrow c\bar{s}$  and  $\tau^+\nu_\tau$ . The process  $e^+e^- \rightarrow W^+W^-$  constitutes a high background at  $m_{H^\pm} \approx M_W$ .

In the SM and the MSSM, the signal and background rates are predicted channel by channel. The corresponding search results can thus be combined for a better overall sensitivity. Furthermore, datasets from different LEP energies and experiments can also be added. The combined LEP data are used to test two hypotheses: the *background-only* (“ $b$ ”) hypothesis, which assumes no Higgs boson to be present in the mass range investigated, and the *signal + background* (“ $s + b$ ”) hypothesis, where Higgs bosons are assumed to be produced according to the model under consideration. A global *test-statistic*  $X$  is constructed [28] which allows the experimental result  $X_{\text{observed}}$  to be classified between the  $b$ -like and  $s + b$ -like situations. It utilizes the number of selected events and various distributions which provide discrimination between signal and background (*e.g.*, the reconstructed mass or  $b$ -tag variables). The test-statistic takes into account experimental details such as detection efficiencies, signal-to-background ratios, resolution functions, and provides a single value for a given model hypothesis (*e.g.*, the test-mass  $m_{H^0}$  in the SM).

To set the scale for  $X$ , a large number of Monte Carlo experiments are generated, separately for the  $b$  and the  $s + b$  hypotheses, and separately for each model hypothesis (*e.g.*,  $m_{H^0}$ ). The resulting distributions of  $X(m_{H^0})$  are normalized to become probability density functions, and integrated to form the confidence levels  $\text{CL}_b(m_{H^0})$  and  $\text{CL}_{s+b}(m_{H^0})$ . The integration starts in both cases from the  $b$ -like end and runs up to  $X_{\text{observed}}$ ; thus  $\text{CL}_b(m_{H^0})$  and  $\text{CL}_{s+b}(m_{H^0})$  express the probabilities that the outcome of an experiment is more  $b$ -like or less  $s + b$ -like, respectively, than the outcome represented by the set of selected events.

The 95% CL lower limit for the SM Higgs mass is defined as the lowest value of the test mass  $m_{H^0}$  which yields\*  $\text{CL}_s(m_{H^0}) = \text{CL}_{s+b}(m_{H^0}) / \text{CL}_b(m_{H^0}) = 0.05$ . The quantity  $1 - \text{CL}_b(m_{H^0})$  is an indicator for a possible signal: a SM Higgs boson with true mass  $m_0$  would produce a pronounced drop in this quantity for  $m_{H^0} \approx m_0$ . Values of  $1 - \text{CL}_b < 5.7 \times 10^{-7}$  would indicate a five-standard deviation ( $5\sigma$ ) discovery.

If values of  $X_{\text{observed}}$  (and thus the integration bounds) are obtained from Monte Carlo simulations of the real experiment, the average expected confidence levels  $\langle 1 - \text{CL}_b(m_{H^0}) \rangle$  and  $\langle \text{CL}_s(m_{H^0}) \rangle$  are obtained. Of particular interest are  $\langle 1 - \text{CL}_b(m_{H^0}) \rangle$  from simulated  $s + b$  experiments and  $\langle \text{CL}_s(m_{H^0}) \rangle$  from simulated  $b$  experiments, since these indicate the expected ranges of sensitivity of the available data set for discovery and exclusion, respectively.

## V. Latest results

We summarize below the search results obtained recently by the LEP Collaborations, the CDF, DØ, and other experiments. Some of the LEP results presented are obtained by combining [29] preliminary data from the four experimental groups [30] according to the procedure outlined above.

### ***Results relevant to the SM and the MSSM:***

(a) For the ***SM Higgs boson***, the confidence levels  $1 - \text{CL}_b$  and  $\text{CL}_s$  obtained from combining the data of the four LEP experiments are shown in Fig. 5 [29]. One can see in the

upper part that the observed behavior of  $1 - \text{CL}_b$  (full line) is compatible with the expected behaviors for background within  $2\sigma$  (light-shaded band). The expected behavior in the presence of a signal (dashed line) indicates that the data have sensitivity for a  $5\sigma$  discovery ( $1 - \text{CL}_b < 5.7 \times 10^{-7}$ ) up to  $m_{H^0} \approx 98$  GeV. In the lower part of the figure, the curves of  $\text{CL}_s$  observed (full line) and expected from background (dashed line) follow each other closely, as anticipated in the absence of a signal. The curves cross the value  $\text{CL}_s = 0.05$  in the vicinity of  $m_{H^0} = 103$  GeV. After cross checking with several test-statistics, the value 102.6 GeV is quoted in Ref. 29 as the 95% CL lower bound for the SM Higgs mass.

At the Tevatron, the SM Higgs boson would be produced primarily by gluon fusion,  $gg \rightarrow H^0$  [31]. However, the signal processes providing best sensitivity to masses below 140 GeV are those where a Higgs boson is produced in association with a  $W^\pm$  or  $Z^0$  boson, or in association with heavy quarks,  $p\bar{p} \rightarrow W^\pm H^0 X$ ,  $Z^0 H^0 X$ ,  $Q\bar{Q}H^0 X$  [32]. The Run I data samples, of about  $110 \text{ pb}^{-1}$  from both CDF and DØ, are far too small for a discovery of the SM Higgs boson but allow upper bounds to be set on the cross section. For  $m_{H^0} > 70$  GeV, these bounds are higher by an order of magnitude at least than the SM prediction [33,34].

(b) For the *MSSM Higgs bosons  $h^0$  and  $A^0$* , the search results are used to test a ‘constrained’ MSSM where universal SUSY-breaking masses  $m_{\text{SUSY}}$  and  $M_2$  are assumed for sfermions and gauginos, respectively, at the electroweak scale. With these assumptions, the number of MSSM parameters is reduced to only six [4,19]. All masses, cross sections, and decay branching ratios can be calculated by fixing  $m_{\text{SUSY}}$ ,  $M_2$ ,  $\tan\beta$ ,  $m_{A^0}$ , the Higgs mixing parameter  $\mu$ , and the trilinear coupling  $A_t$  which controls stop mixing. The top mass has also an impact on the predictions through loop corrections.

Although more general parameter scans have been reported [35,36], most interpretations of the results are limited to less general scenarios (*e.g.*, those proposed in Ref. 20), where some of the parameters are fixed:  $m_{\text{SUSY}}=1 \text{ TeV}/c^2$ ,  $M_2=1.6 \text{ TeV}/c^2$ ,  $\mu = -100 \text{ GeV}$ , and  $m_t = 175 \text{ GeV}$ . Two

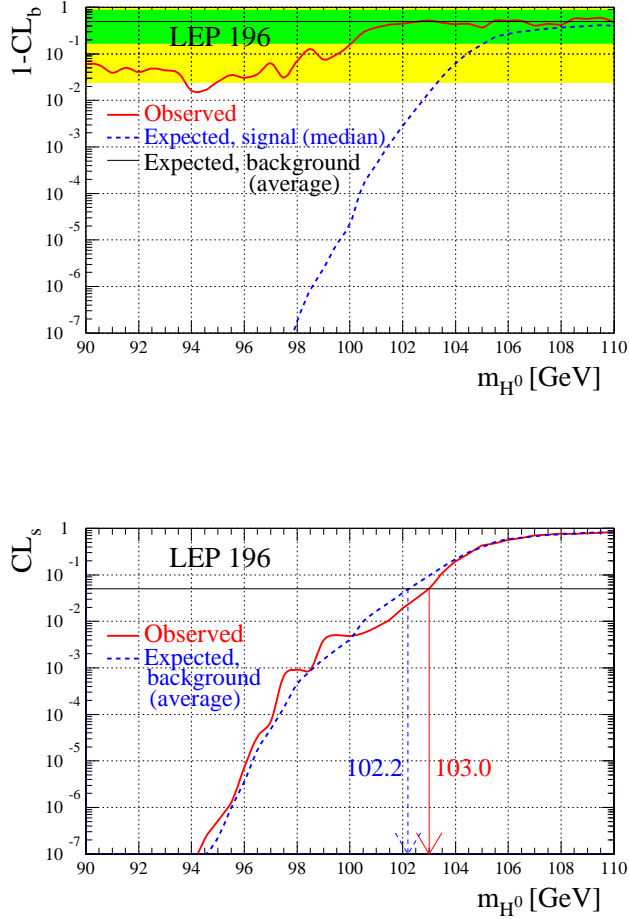


**Figure 5:** The confidence levels  $1 - CL_b$  (upper) and  $CL_s$  (lower part), observed and expected, as a function of the test mass  $m_{H^0}$ , obtained from combining [29] preliminary data of the four LEP experiments. The dark (light) shaded areas represent the  $\pm$ one- (two-) standard deviation bands around the expected average (0.5) from simulated *background only* experiments.

separate cases are considered, with  $A_t = 0$  and  $\sqrt{6}$  TeV, which correspond to *no mixing* and *large stop-mixing*. The remaining parameters,  $m_{A^0}$  and  $\tan \beta$ , are scanned independently.

The current LEP limits in the MSSM parameter space [29], valid for *large mixing*, are shown in Fig. 6 in the  $(m_{h^0}, \tan \beta)$  and  $(m_{A^0}, \tan \beta)$  projections (for *no mixing* the available parameter space is more restricted). The current 95% CL bounds are:

$m_{h^0} > 84.3$  GeV,  $m_{A^0} > 84.5$  GeV. Furthermore, values of  $\tan\beta$  from 0.8 to 1.9 are excluded for the parameter sets considered; however, that exclusion can be reduced considerably in other scenarios [37].

The CDF experiment has searched for the process  $p\bar{p} \rightarrow b\bar{b}X \rightarrow b\bar{b}b\bar{b}$  [33] where a particle  $X(\equiv h^0, H^0, A^0)$  is radiated from a  $b$  quark and decays subsequently to  $b\bar{b}$ . This process is enhanced in the MSSM at large  $\tan\beta$  where the Yukawa coupling to the  $b$  quark is large. The domains excluded by CDF are indicated in Fig. 6 together with the limits from LEP.

***Interpretations in models beyond the SM and the MSSM:***

Any model, to be acceptable, has to reproduce the available precision electroweak data. 2HD models with any number of additional singlet or doublet fields satisfy this criterion. This has been demonstrated [38] for 2HD models of class II where the “up” and “down” fermions couple to separate Higgs doublets. In the case of higher representations (*e.g.*, triplet fields) the parameters can also be tuned to obtain agreement, in particular to preserve the value of  $\rho = M_W^2/M_Z^2 \cos^2\theta_W$  and to avoid excessive rates of flavor-changing neutral currents. Search results are discussed below in theoretical contexts which are more general than the SM and the MSSM.

(a) The searches for  $e^+e^- \rightarrow h^0 Z^0$  and  $h^0 A^0$  have been used to derive ***model-independent bounds*** for the rates of *generic processes* where  $h^0$  and  $A^0$  can be any  $CP$ -even and  $CP$ -odd scalar particles [36,40]. In deriving these limits it is generally assumed that the decay properties of the generic particles are identical to those of the SM Higgs boson. Models with  $CP$  violation [39] and non-SM decay properties have also been addressed [40].

(b) The searches for ***charged Higgs bosons*** are guided by predictions of 2HD models. The mass  $m_{H^\pm}$  is not constrained. In the LEP searches [41] it is assumed that the decay modes  $H^+ \rightarrow c\bar{s}$  and  $\tau^+\nu_\tau$  fully exhaust the decay width, but the relative branching ratio is unknown. They therefore include the  $e^+e^- \rightarrow H^+H^-$  final states  $(c\bar{s})(\bar{c}s)$ ,  $(\tau^+\nu_\tau)(\tau^-\bar{\nu}_\tau)$  and  $(c\bar{s})(\tau^-\bar{\nu}_\tau) + (\bar{c}s)(\tau^+\nu_\tau)$ . The current combined limits from LEP [29] are reproduced in Fig. 7 as a function of the branching

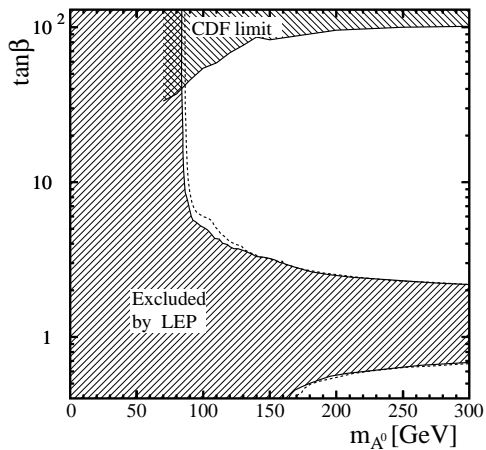
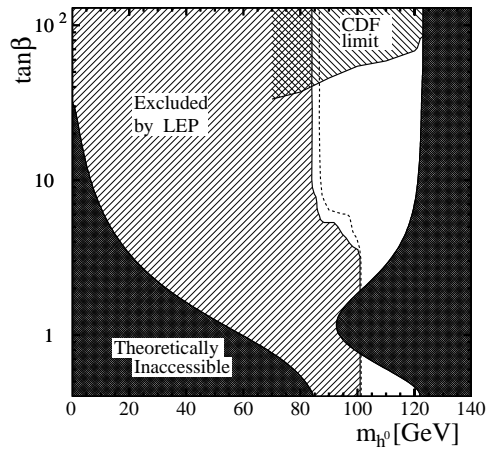


**Figure 6:** The 95% CL bounds on  $m_{h^0}$ ,  $m_{A^0}$ , and  $\tan\beta$ , for the case of large mixing, from combining the data of the four LEP experiments up to  $\sqrt{s} = 196$  GeV [29]. The dashed lines indicate the expected limits. The exclusions at large  $\tan\beta$  from the CDF experiment [33] are also indicated.

ratio  $B(H^+ \rightarrow \tau^+ \nu_\tau)$ . The lowest value, independent of the branching ratio, is currently 77 GeV.

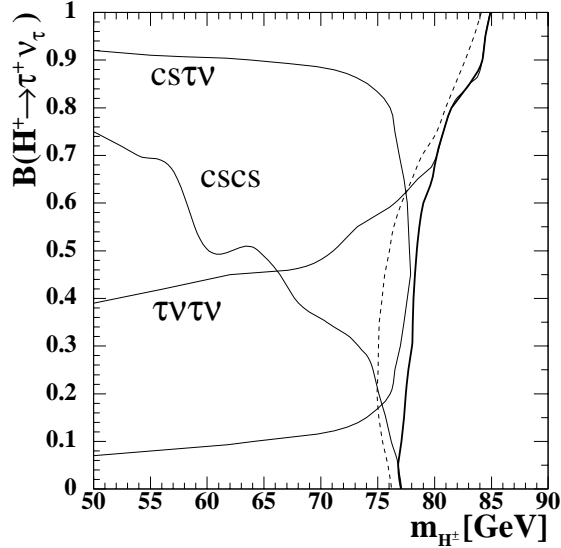


**Figure 7:** The 95% CL bounds on  $m_{H^\pm}$  as a function of the branching ratio  $B(H^+ \rightarrow \tau^+ \nu_\tau)$ , from combining the data collected by the LEP experiments at energies up to 196 GeV [29]. The expected exclusion limit is indicated by the dashed line and the observed limits, channel-by-channel (light) and total (heavy), by the full lines.

At the Tevatron, charged Higgs bosons may be produced in the decay of the top quark,  $t \rightarrow bH^+$ . While the SM requires the top quark to decay almost exclusively via  $t \rightarrow bW^+$ , in 2HD models the process  $t \rightarrow bH^+$  may compete with the SM process if  $m_{H^+} < m_t - m_b$  and if  $\tan \beta$  is either large ( $> 30$ ) or less than one. To search for  $H^\pm$ , the DØ experiment has adopted an indirect “disappearance technique [42],” optimized for the detection of the SM background process  $t \rightarrow bW^+$ . The CDF Collaboration reported on a direct search for the process  $t \rightarrow H^+ b \rightarrow \tau^+ \nu_\tau b$  [43] and on an indirect approach [44] in which the rate of di-leptons and lepton+jets in  $t\bar{t}$  decay is compared to the SM prediction. The 2HD model of class II is assumed by both collaborations, and that the  $H^+$  decays into three channels: (i)  $c\bar{s}$ , which is dominant at low  $\tan \beta$  and

small  $m_{H^\pm}$ , (ii)  $t^*b \rightarrow W^+b\bar{b}$ , dominant at low  $\tan\beta$  and for  $m_{H^\pm} \approx m_t + m_b$  [27], and (iii)  $\tau^+\nu_\tau$ , dominant at high  $\tan\beta$ . The results are summarized in Fig. 8, where the LEP limits of Fig. 7 are also reproduced. All these limits are subject to potentially large theoretical uncertainties [45].

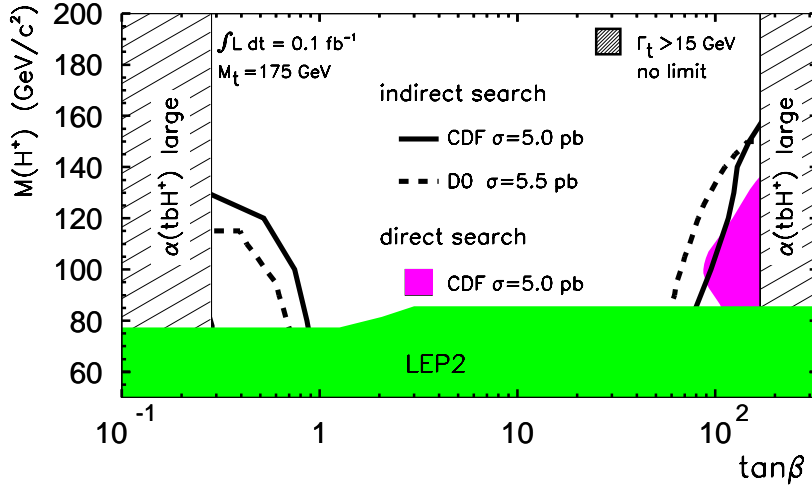


**Figure 8:** Summary of the 95% CL exclusions in the  $(m_{H^+}, \tan\beta)$  plane obtained by the DØ [42] and CDF [43] collaborations, using various indirect and direct observation techniques. The limits quoted by the two collaborations were obtained assuming slightly different  $t\bar{t}$  cross sections and using different statistical procedures. The LEP limits from Fig. 7 are also reproduced.

Indirect limits in the  $(m_{H^\pm}, \tan\beta)$  plane can also be derived using experimental bounds on the branching ratio of the flavor-changing neutral current process  $b \rightarrow s\gamma$ . In the SM, this process is induced by virtual  $W^\pm$  exchange and gives rise to a branching ratio of  $(3.28 \pm 0.33) \times 10^{-4}$  [46]. In 2HD models of class II, the branching ratio is increased [47] by contributions from charged Higgs bosons. Thus, the experimental 95% CL upper bound of  $4.5 \times 10^{-4}$  obtained by the CLEO Collaboration [48] can be translated into a lower bound on  $m_{H^\pm}$ ,

which is in the vicinity of 300 GeV and depends moderately on  $\tan\beta$ . Less stringent limits are obtained from measurements of the  $b \rightarrow s\gamma$  and  $b \rightarrow \tau^-\bar{\nu}_\tau X$  rates and from tau-lepton decay properties at LEP [49]. All these indirect bounds are model-dependent and may be invalidated, *e.g.*, by sparticle loops or anomalous couplings.

(c) Higgs bosons with ***double-electric charge***,  $H^{\pm\pm}$ , are predicted by several models [50,19] *e.g.*, with triplet scalar fields. The OPAL Collaboration has searched for the process  $Z^0 \rightarrow H^{++}H^{--}$  in final states with four prompt electrons or muons. An alternative selection, sensitive to long-lived  $H^{\pm\pm}$  and giving rise to isolated tracks with ionization energy loss typical for two electron charges, was also used. By combining the two searches,  $H^{\pm\pm}$  bosons with mass less than  $M_Z/2$  could almost completely be excluded [51].

(d) The addition of a ***singlet scalar field*** to the MSSM [52], gives rise to two additional neutral scalars, one  $CP$ -even and one  $CP$ -odd. The radiative corrections to the masses are similar to those in the MSSM and arguments of perturbative continuation to the GUT scale lead again to an upper bound of about 135-140 GeV for the mass of the lightest neutral  $CP$ -even scalar. The DELPHI Collaboration has used the searches for neutral Higgs bosons to constrain such models [53].

(e) Higgs bosons can be produced by ***Yukawa processes*** in which they are radiated from a massive fermion, *e.g.*,  $b$  or  $\tau^\pm$ . The CDF search for this process [33] has already been discussed in the MSSM context of Fig. 6. In a broader context, this process can be dominant in regions of the 2HD model space where the “standard” processes are suppressed. The LEP1 data have recently been reanalyzed [54], searching specifically for  $b\bar{b}b\bar{b}$ ,  $b\bar{b}\tau^+\tau^-$ , and  $\tau^+\tau^-\tau^+\tau^-$  final states.

(f) Decays into ***“invisible” particles*** (weakly interacting neutral particles) may occur, *e.g.*, in the MSSM with  $R$ -parity conservation, if the Higgs bosons decay to pairs of neutralinos [55]. In a different context, Higgs bosons could also decay into pairs of massless Goldstone bosons or Majorons [56]. In Higgs-strahlung,  $e^+e^- \rightarrow h^0 Z^0$ , the mass of the invisible Higgs boson can be inferred from the  $Z^0$  boson which is

reconstructed in the  $Z^0 \rightarrow e^+e^-$ ,  $\mu^+\mu^-$ , and  $q\bar{q}$  final states, and using the beam energy constraint. Assuming the SM production rate, the LEP experiments exclude the existence a Higgs boson of mass less than about 95 GeV decaying exclusively to invisible final states [57].

(g) **Photonic final states** from the processes  $Z^0/\gamma^* \rightarrow H^0\gamma$  and  $H^0 \rightarrow \gamma\gamma$  do not occur in the SM at the tree level, but may be present at a low rate due to  $W^\pm$  and top-quark loops [58]. Additional loops, *e.g.*, from SUSY particles, would increase the rates only slightly [59], but models with anomalous couplings predict enhancements by orders of magnitude. Searches for the processes  $e^+e^- \rightarrow (H^0 \rightarrow b\bar{b})\gamma$ ,  $(H^0 \rightarrow \gamma\gamma)q\bar{q}$ , and  $(H^0 \rightarrow \gamma\gamma)\gamma$  have been used to set model-independent limits on such anomalous couplings. They were also used to constrain very specific models leading to an enhanced  $H^0 \rightarrow \gamma\gamma$  rate, such as the “fermiophobic” 2HD model of class I [60], where all fermions are assumed to couple to the same scalar field, and the couplings can thus be suppressed simultaneously by appropriate parameter choices. The searches at LEP [61] exclude a fermiophobic Higgs boson with mass less than about 95 GeV. At the Tevatron, limits of 82 GeV and 78.5 GeV are obtained by CDF and DØ, respectively [33,62].

**Note: Very Recent Results (March 2000)**

*Very recently, the LEP Higgs working group updated their results including all LEP data collected in 1999 [63]. They report no indication for a signal. The new 95% CL mass bounds, replacing the ones quoted in this section, are the following. For the SM Higgs boson,  $m_{H^0} > 107.7$  GeV; for the  $h^0$  and  $A^0$  bosons of MSSM,  $m_{h^0} > 88.3$  GeV and  $m_{A^0} > 88.4$  GeV; finally, for charged Higgs bosons in 2HD models,  $m_{H^\pm} > 78.6$  GeV.*

**VI. Outlook**

The LEP collider is scheduled to stop producing data in the year 2000. At the Tevatron, the Run I sensitivity is rather limited for Higgs boson searches, but a powerful luminosity upgrade is in preparation. Performance studies [8] provide a high motivation for collecting large data samples in excess of  $10 \text{ fb}^{-1}$  per experiment. Such samples will extend the combined

sensitivity of CDF and DØ well beyond the LEP reach and allow large domains in the MSSM parameter space to be investigated.

The Large Hadron Collider (LHC) will deliver proton-proton collisions at 14 TeV energy in the year 2005. The ATLAS and CMS detectors have been optimized for Higgs boson searches [9]. The discovery of the SM Higgs boson will be possible over the full canonical mass range between 100 GeV and 1 TeV. This broad range is covered by a variety of production and decay processes. The LHC experiments will provide full coverage of the MSSM parameter space *via* their searches for the  $h^0$ ,  $H^0$ ,  $A^0$ , and  $H^\pm$  bosons and by detecting the  $h^0$  boson in cascade decays of SUSY particles. The discovery of several Higgs bosons is possible over extended domains of the parameter space. Decay branching fractions can be determined, and masses measured with accuracies between  $10^{-3}$  (at 400 GeV mass) and  $10^{-2}$  (at 700 GeV).

It is conceivable that a high-energy  $e^+e^-$  linear collider will be realized after the year 2010. Initially it could run at energies up to 500 GeV, with 1 TeV and more in perspective [10]. One of the prime goals of such a collider is to extend the precision measurements, typical of  $e^+e^-$  colliders, to the Higgs sector. The Higgs couplings to fermions and vector bosons can be measured through production cross sections and decay branching ratios, with precisions of a few percent. The MSSM parameters can be studied in great detail. At the highest collider energies and luminosities, the self-coupling of the Higgs fields can be studied directly through final states with two Higgs bosons [64].

At a future  $\mu^+\mu^-$  collider [11], the Higgs bosons can be generated as  $s$ -channel resonances. Mass measurements with precisions of a few MeV would be possible and the widths could be obtained directly from Breit-Wigner scans. The heavy  $CP$ -even and  $CP$ -odd Higgs bosons  $H^0$  and  $A^0$ , degenerate over most of the MSSM parameter space, could be disentangled experimentally.

Finally, if Higgs bosons are not discovered at the TeV scale, both the LHC and the future lepton colliders will be in a position to test alternative theories of electroweak symmetry breaking

such as those with strongly interacting vector bosons [65], expected in theories with dynamical symmetry breaking [66].

## Notes and References

- \* The ratio  $CL_s$  replaces  $CL_{s+b}$  in order to avoid situations where a downward fluctuation of the event count would exclude even the  $b$ -like hypothesis. In such situations, the exclusion of the  $s + b$  hypothesis would incorrectly appear as an exclusion of a signal for which there is insufficient experimental sensitivity.
1. S.L. Glashow, Nucl. Phys. **20**, 579 (1961);  
S. Weinberg, Phys. Rev. Lett. **19**, 1264 (1967);  
A. Salam, *Elementary Particle Theory*, ed.: N. Svartholm, Almquist, and Wiksells, Stockholm, 1968;  
S. Glashow, J. Iliopoulos, and L. Maiani, Phys. Rev. **D2**, 1285 (1970).
  2. P.W. Higgs, Phys. Rev. Lett. **12**, 132 (1964); Phys. Rev. **145**, 1156 (1966);  
F. Englert and R. Brout, Phys. Rev. Lett. **13**, 321 (1964);  
G.S. Guralnik, C.R. Hagen, and T.W. Kibble, Phys. Rev. Lett. **13**, 585 (1964).
  3. J. Wess, B. Zumino, Nucl. Phys. **B70**, 39 (1974); *idem*, Phys. Lett. **49B**, 52 (1974);  
P. Fayet, Phys. Lett. **69B**, 489 (1977); *ibid.* **84B** 421, (1979); **86B**, 272 (1979);  
H.E. Haber, *Supersymmetry*, elsewhere in this *Review*.
  4. K. Inoue, A. Kakuto, H. Komatsu, and S. Takeshita, Prog. Theor. Phys. **68**, 927 (1982); *ibid.* **70**, 330 (1983); *ibid.* **71**, 413 (1984);  
H.E. Haber and G.L. Kane, Phys. Rep. **C117**, 75 (1985).
  5. Y. Okada, M. Yamaguchi, and T. Yanagida, Theor. Phys. **85**, 1 (1991);  
H. Haber and R. Hempfling, Phys. Lett. **66**, 1815 (1991);  
J. Ellis, G. Ridolfi, and F. Zwirner, Phys. Lett. **B257**, 83 (1991);  
R. Barbieri and M. Frigeni, Phys. Lett. **B258**, 395 (1991).
  6. P.J. Franzini and P. Taxil, in *Z physics at LEP 1*, CERN 89-08 (1989).
  7. For complete documentation of published results, the reader should consult the Particle Listings in this *Review* and in the 1998 Edition (Eur. Phys. J. **C3**, 1 (1998)).
  8. Tevatron Run II workshop,  
<http://fnth37.fnal.gov/higgs.html>;  
M. Spira, hep-ph/9810289;

- J.S. Conway, FERMILAB-CONF-99/156-E.
9. ATLAS TDR on Physics performance, Vol. II, Chap. 19, *Higgs Bosons* (1999); CMS TP, CERN/LHC 94-38 (1994)..
  10. E. Accomando *et al.*, Physics Reports **299**, 1 (1998);  
H. Murayama and M.E. Peskin, Ann. Rev. Nucl. and Part. Sci. **46**, 583 (1996); ACFA Workshop, KEK Report 99-12, 1999;  
K. Hübner, *Future Accelerators*, Proceedings of ICHEP'98, Vancouver, Canada, July 1998;  
G. Borisov and F. Richard, hep-ph/9905413;  
M. Battaglia, hep-ph/9910271.
  11. B. Autin, A. Blondel, and J. Ellis (eds.), CERN 99-02;  
C.M. Ankenbrandt *et al.*, Phys. Rev. ST Acc. Beams **2**, 081001 (1999).
  12. N. Cabibbo, L. Maiani, G. Parisi, and R. Petronzio, Nucl. Phys. **B158**, 295 (1979);  
R. Dashen and H. Neuberger, Phys. Rev. Lett. **50**, 1897 (1983).
  13. M. Lindner, M. Sher, and H.W. Zaglauer, Phys. Lett. **B228**, 139 (1989);  
M. Sher, Phys. Lett. **B317**, 159 (1993); *ibid.* **331B**, 448 (1994);  
G. Altarelli and I. Isidori, Phys. Lett. **B337**, 141 (1994);  
J.A. Casas, J.R. Espinosa, and M. Quirós, Phys. Lett. **B342**, 89 (1995).
  14. T. Hambye and K. Riesselmann, Phys. Rev. **D55**, 7255 (1997).
  15. J. Erler and P. Langacker, *Electroweak Model and Constraints on New Physics*, elsewhere in this *Review*.
  16. G. Quast, \*ew-fits\*.
  17. M. Carena, M. Quiros, and C.E.M. Wagner, Nucl. Phys. **B461**, 407 (1996);  
H. Haber, R. Hempfling, and A. Hoang, Z. Phys. **C75**, 539 (1997);  
S. Heinemeyer, W. Hollik, and G. Weiglein, Phys. Lett. **B455**, 179 (1999); *idem*, Eur. Phys. J. **C9**, 343 (1999).
  18. M. Carena, S. Pokorski, and C. Wagner, Nucl. Phys. **B406**, 45 (1993);  
V. Barger, M.S. Berger, and P. Ohmann, Phys. Rev. **D47**, 1093 (1993);  
M. Carena and C. Wagner, Nucl. Phys. **B452**, 45 (1995).
  19. J.F. Gunion, H.E. Haber, G.L. Kane, and S. Dawson, *The Higgs Hunter's Guide* (Addison-Wesley) 1990.

20. M. Carena *et al.*, LEP2 Workshop, CERN 96-01, (1996) Vol. 1, p. 351.
21. J. Ellis, M.K. Gaillard, and D.V. Nanopoulos, Nucl. Phys. **B106**, 292 (1976);  
B.L. Ioffe and V.A. Khoze, Sov. J. Nucl. Phys. **9**, 50 (1978).
22. E. Gross, B.A. Kniehl, and G. Wolf, Z. Phys. **C63**, 417 (1994); erratum *ibid.* **C66**, 32 (1995).
23. D.R.T. Jones and S.T. Petcov, Phys. Lett. **84B**, 440 (1979);  
G. Altarelli, B. Mele, and F. Pitolli, Nucl. Phys. **B287**, 205 (1987);  
W. Kilian, M. Krämer, and P.M. Zerwas, Phys. Lett. **B373**, 135 (1996).
24. J.F. Gunion and H.E. Haber, Nucl. Phys. **B272**, 1 (1986);  
*ibid.* **B278**, 449 (1986); *ibid.* **B307**, 445 (1988); erratum:  
*ibid.* **B402**, 567 (1993).
25. A. Brignole, J. Ellis, G. Ridolfi, and F. Zwirner, Phys. Lett. **B271**, 123 (1991).
26. A. Djouadi, M. Spira, P.M. Zerwas, Z. Phys. **C70**, 675 (1996).
27. A. Djouadi *et al.*, Z. Phys. **C70**, 435 (1996);  
E. Ma, D.P. Roy, and J. Wudka, Phys. Rev. Lett. **80**, 1162 (1998).
28. LEP Higgs working group: CERN-EP/98-046, CERN-EP/99-060;  
\*lephiggs-1\*.
29. LEP Higgs working group: \*lephiggs-2\*.
30. \*ALEPH 99-084\*, \*ALEPH 99-070\*, \*DELPHI 99-86\*,  
\*DELPHI 99-95\*, \*DELPHI 99-92\*, M. Acciarri *et al.*,  
Phys. Lett. **B461**, 376 (1999); *idem* **B466**, 71 (1999);  
CERN-EP/99-145; \*OPAL-PN/99-373\*, \*OPAL-PN/99-414\*, CERN-EP/99-096.
31. H. Georgi, S. Glashow, M. Machacek, and D.V. Nanopoulos, Phys. Rev. Lett. **40**, 692 (1978);  
M. Spira, A. Djouadi, D. Graudenz and P.M. Zerwas, Nucl. Phys. **B453**, 17 (1995).
32. S.L. Glashow, D.V. Nanopoulos, and A. Yildiz, Phys. Rev. **D18**, 1724 (1978);  
Z. Kunszt, Nucl. Phys. **B247**, 339 (1984);  
D. Dicus and S. Willenbrock, Phys. Rev. **D39**, 751 (1989).
33. Xin Wu, FERMILAB-CONF-99/053-E;  
J.A. Walls, FERMILAB-CONF-99/263-E.

34. F. Abe *et al.*, Phys. Rev. Lett. **79**, 3819 (1997); *ibid.*, **81**, 5748 (1998);  
W.-M. Yao, FERMILAB-CONF-99/100.
35. R. Barate *et al.*, Phys. Lett. **B440**, 419 (1998); \*DELPHI 98-124\*.
36. G. Abbiendi *et al.*, Eur. Phys. J. **C7**, 407 (1999).
37. G. Weiglein, S. Heinemeyer, W. Hollik, hep-ph/9909540;  
M. Carena *et al.*, hep-ph/9912223.
38. P. Chankowski, M. Krawczyk, J. Zochowski,  
hep-ph/9905436.
39. J.F. Gunion, B. Grzadkowski, H.E. Haber, J. Kalinowski,  
Phys. Rev. Lett. **79**, 982 (1997).
40. \*ALEPH 99-053\*, \*DELPHI 99-86\*; \*OPAL-PN/99-416\*.
41. \*ALEPH 99-070\*, CERN-EP/99-011, CERN-EP/98-149,  
\*DEPPHI 99-92\*, M. Acciarri *et al.*, Phys. Lett. **B466**, 71  
(1999); \*OPAL-PN/99-373\*, \*OPAL-PN/99-414\*.
42. B. Abbott *et al.*, Phys. Rev. Lett. **82**, 4975 (1999).
43. F. Abe *et al.*, Phys. Rev. Lett. **79**, 357 (1997);  
T. Affolder *et al.*, hep-ex/9912013.
44. B. Bevensee, FERMILAB-CONF-98/155-E.
45. J.A. Coarasa, J. Guach, and J. Solá, hep-ph/9903212;  
J.A. Coarasa, J. Guach, J. Solá, and W. Hollik,  
hep-ph/9808278;  
F.M. Borzumati and A. Djouadi, hep-ph/9806301.
46. K. Chetyrkin *et al.*, Phys. Lett. **B400**, 206 (1997); *idem*  
Phys. Lett. **B425**, 414 (1998);  
A. Kagan and M. Neubert, Eur. Phys. J. **C7**, 5 (1999).
47. R. Ellis *et al.*, Phys. Lett. **B179**, 119 (1986);  
V. Barger, J. Hewett, and R. Phillips, Phys. Rev. **D41**,  
3421 (1990).
48. M.S. Alam *et al.*, Phys. Rev. Lett. **74**, 2885 (1995);  
S. Ahmed *et al.*, hep-ex/9908022.
49. O. Adriani *et al.*, Phys. Lett. **B317**, 637 (1993);  
D. Buskulic *et al.*, Phys. Lett. **B343**, 444 (1995);  
W. Adam *et al.*, Z. Phys. **C72**, 207 (1996);  
R. Barate *et al.*, Phys. Lett. **B429**, 169 (1998);  
K. Ackerstaff *et al.*, Eur. Phys. J. **C8**, 3 (1999).
50. G.B. Gelmini and M. Roncadelli, Phys. Lett. **99B**, 411  
(1981);  
R.N. Mohapatra and J.D. Vergados, Phys. Rev. Lett. **47**,  
1713 (1981);  
V. Barger, H. Baer, W.Y. Keung, and R.J.N. Phillips,  
Phys. Rev. **D26**, 218 (1982).

51. P.D. Acton *et al.*, Phys. Lett. **B295**, 347 (1992).
52. P. Fayet, Nucl. Phys. **B90**, 104 (1975);  
S.A. Abel, S. Sarkar, P.L. White, Nucl. Phys. **B454**, 663 (1995);  
S.F. King, P.L. White, Phys. Rev. **D53**, 4049 (1996).
53. \*DELPHI 99-97\*.
54. \*ALEPH PA13-027\*; \*DELPHI 99-76\*.
55. A. Djouadi, P. Janot, J. Kalinowski, and P.M. Zerwas, Phys. Lett. **B376**, 220 (1996).
56. Y. Chikashige, R.N. Mohapatra, and P.D. Peccei, Phys. Lett. **98B**, 265 (1981);  
F. de Campos, O.J.Éboli, J. Rosiek, and J.W.F. Valle, Phys. Rev. **D55**, 1316 (1997).
57. \*ALEPH 99-069\*; \*DELPHI 99-83\*; \*L3 Note 2435\*; \*OPAL-PN/99-399\*.
58. J. Ellis, M.K. Gaillard, and D.V. Nanopoulos, Nucl. Phys. **B106**, 292 (1976);  
R.N. Cahn, M.S. Chanowitz, and N. Fleishon, Phys. Lett. **B82**, 113 (1997);  
J. Leveille, Phys. Lett. **B83**, 123 (1997);  
A.I. Vainshtein *et al.*, Sov. J. Nucl. Phys. **30**, 711 (1979);  
A. Barroso, J. Pulido, J.C. Romão, Nucl. Phys. **B267**, 509 (1986);  
A. Abbasabadi *et al.*, Phys. Rev. **D52**, 3919 (1995).
59. G. Gamberini, G.F. Giudice, and G. Ridolfi, Nucl. Phys. **B292**, 237 (1987);  
R. Bates, J.N. Ng, and P. Kalyniak, Phys. Rev. **D34**, 172 (1986);  
K. Hagiwara, R. Szalapski, and D. Zeppenfeld, Phys. Lett. **B318**, 155 (1993);  
O.J.P. Éboli, M.C. Gonzalez-Garcia, S.M. Lietti, and S.F. Novaes, Phys. Lett. **B434**, 340 (1998).
60. A.G. Akeroyd, Phys. Lett. **B368**, 89 (1996);  
H. Haber, G. Kane, and T. Stirling, Nucl. Phys. **B161**, 493 (1979) 493.
61. \*ALEPH 99-054\*, \*DELPHI 99-72\*, CERN-EP/99-058, \*L3 Note 2429\*; G. Abbiendi *et al.*, Phys. Lett. **B464**, 311 (1999).
62. B. Abbott *et al.*, hep-ex/9902028.
63. \*lephiggs-3\*.
64. G.J. Gounaris, F. Renard, D. Schildknecht, Phys. Lett. **83B**, 191 (1979);  
V. Barger, T. Han, R.J.N. Phillips, Phys. Rev. **D38**, 2766 (1988);

- F. Boudjema and E. Chopin, Z. Phys. **C37**, 85 (1996);  
A. Djouadi, W. Kilian, M. Mühlleitner, and P.M. Zerwas,  
Eur. Phys. J. **C10**, 27 (1999).
65. B.W. Lee, C. Quigg, and H.B. Thacker, Phys. Rev. **D16**,  
1519 (1977);  
R.S. Chivukula *et al.*, hep-ph/9503202,;  
C. Yuan, hep-ph/9712513;  
M. Chanowitz, hep-ph/9812215.
66. S. Weinberg, Phys. Rev. **D13**, 974 (1976); *ibid.* **D19**, 1277  
(1979);  
L. Susskind, Phys. Rev. **D20**, 2619 (1979).